Letter

Pseudogap in hole-doped cuprates: Possible insights from the Kondo effect

J. R. Cooper
Cavendish Laboratory, University of Cambridge, J.J. Thomson Avenue CB3 0HE, United Kingdom

(Received 2 August 2021; revised 1 December 2021; accepted 16 December 2021; published 3 January 2022)

The "states-non-conserving" fermion density of states (DOS), deduced from the specific heat of hole-doped cuprates, could arise from a Kondo or heavy fermionlike DOS being suppressed by antiferromagnetic spin fluctuations. The large Fermi surface predicted by band theory and observed experimentally is still expected for zero pseudogap but with an effective mass corresponding to a Kondo temperature $T_K \simeq 800$ K. A finite pseudogap could divide it into Fermi arcs. Theoretical results for the asymmetric Anderson model can account for the experimental Wilson ratio.

DOI: 10.1103/PhysRevB.105.L041102

One of the unsolved questions for cuprate superconductors in addition to the pairing mechanism and the linear temperature (T) dependence of the electrical resistivity is the origin of the pseudogap (PG) in samples with a certain number of holes (p) per CuO_2 unit. The PG lowers the superconducting condensation energy [1,2], the superfluid density, e.g., Ref. [3], and an important practical property, the irreversibility field [4] where the electrical resistivity first becomes nonzero, even though the zero-field transition temperature initially stays high. Many researchers focus on a $T^* - p$ "phase diagram" and a $T^*(p)$ line, ascribed to the onset of a PG, that goes to zero as p is increased to $p_{\rm crit}$ [5]. Careful experiments reveal anomalies in several physical properties at, or near T^* [5], but the values of T^* and the size of the anomalies are probably too small to account for the PG. For example, the small [6] charge-density wave (CDW) anomalies for underdoped (UD) samples may be linked [7] to the Fermi arcs, detected by angle-resolved photoemission (ARPES), that are caused by the preexisting PG. Abrupt changes in magnetic anisotropy of $YBa_2Cu_3O_{6+x}$ (YBCO) crystals defining a nematic $T^*(p)$ line [8], that also extrapolates to zero at $p_{\rm crit}$, are also small—typically, 0.5% of the average in-plane spin susceptibility for $\Delta T \sim 50$ K. Here we retain the idea, reviewed along with many experimental facts in Ref. [9], that the PG is best described as a T-independent energy scale E_G that varies strongly with p. We argue that it might be caused by low-energy antiferromagnetic (af) spin fluctuations giving a deep dip in a Kondo or heavy fermionlike density of states (DOS) at the Fermi energy (E_F).

Analysis of the specific heat of YBCO [10], $Bi_2Sr_2CaCu_2O_{8+x}$ (Bi2212) [2] at different oxygen levels (x), and $La_{2-y}Sr_yCuO_4$ (LSCO) [2]. In terms of a "states-non-conserving" V-shaped fermion DOS [1], centered at E_F, in an otherwise flat band as sketched in Fig. 1(a), gives intriguing insights. It has has some deficiencies because (i) the large thermoelectric power (TEP) and its scaling with E_G [11] require electron-hole asymmetry, (ii) the detection of quantum oscillations and Fermi arcs implies that there is a small residual DOS at E_F and (iii) Y^{89} NMR Knight-shift data for overdoped (OD) Y(Ca)BCO [12] show a fall of up to 20% in the spin susceptibility, $\chi_s(T)$, at higher T rather than the constant value expected for a flat band, there are also small deviations from flat-band behavior for OD Bi2212 [2]. On the other hand Cu NMR data for La-doped Bi2201 [13] seem to be consistent with a flat band. They also show that the PG is not affected by fields up to 44 T, and that the residual DOS is much larger in Bi2201. The main features of this first-order phenomenological analysis are as follows.

(A) E_G falls linearly with p as $J_{af}(1 - p/p_{\rm crit})$ disappearing abruptly at $p_{\rm crit} = 0.17$–0.19 [1], where $J_{af}/k_B =$ 1200–1500 K is similar to the af interaction $J_{af}/k_B = 1700$ K [14] in the corresponding parent insulator with $p = 0$ and k_B is Boltzmann's constant.

(B) Plots of $S_e(T, p)$ vs T, where $S_e(T, p)$ is the nonphonon, electronic contribution to the entropy, are approximately linear and parallel at higher T, e.g., Fig. 1(b) of Ref. [2], and Fig. 5 of Ref. [10], or Figs. 1 and 2 of the Supplemental Material (SM) [15]. $S_e(T, p)$ curves for $p < p_{\rm crit}$ have lower entropy at all T, and there is no sign of the entropy "coming back" up to, at least, 200 K for Bi-2212 and 300 K for YBCO. This behavior is consistent with a recent comprehensive NMR paper [16]. For fermions with an energy- (E-) dependent DOS we expect $S_e(T) \alpha T\chi_s(T)$ because both depend on the number of states within the thermal window $|E - E_F| \lesssim 2k_BT$. $T\chi_s(T)$ curves for Bi2212 are parallel up to 400 K, see Fig. 13(b) of Ref. [2] or Fig. 3 in the SM [15] as are plots of $T\chi_s(T)$ for $Y_{0.8}Ca_{0.2}Ba_2Cu_3O_{6+x}$, also up to 400 K [17], after allowing for an x-independent Curie or Curie-Weiss term. The difference between a states-conserving CDW or superconductorlike DOS and a V-shaped gap is shown by the results of model calculations of $S_e(T)$ in Fig. 4 of the SM [15].

(C) Plots of $S_e(T_0)$ vs p and $k_BT_0\chi_s(T_0)$ vs p at temperatures T_0 show anomalously large increases of $\approx k_B$ and $0.3\mu_B^2$ per added hole, respectively [2], where μ_B is the Bohr magneton. For $p < p_{\rm crit}$, this is caused by the p dependence of the PG and is consistent with the Wilson ratio discussed later. For $p > p_{\rm crit}$, they peak near $p = 0.25$ before falling again, but this

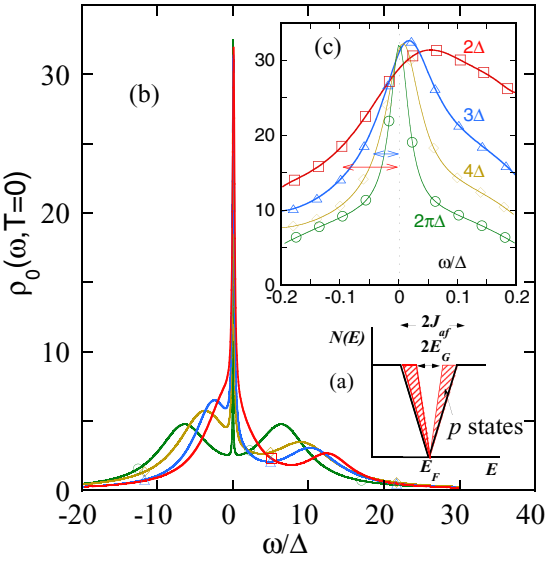

FIG. 1. (a) Fermion DOS [1] used to rationalize specific-heat data. (b) and (c), taken from Ref. [18] with permission, triple peak structure in the spectral density $\rho_0(\omega, T = 0)$ calculated using NRG theory for the single orbital, asymmetric Anderson model with $S_{\rm imp} = 1/2$ for various values of $-E_0/\Delta = 2\pi$, 4, 3, and 2. Here we estimate $-E_0/\Delta = 2.3$ for all the Cu ions in Bi2212. The horizontal arrows show $T_K/\Delta/2$ for $-E_0/\Delta = 2$ and 3 from Ref. [18]. Here the factor 2 ensures consistency between Eq. (1) [19] and Ref. [18], details are given in Ref. [15].

interesting result has only been established experimentally for LSCO [2].

(D) $p_{\rm crit}$ seems to be determined by the product of J_{af} and the DOS at high energy [2]. In contrast to points A–C, this is not expected in the present picture because here J_{af} in the parent compound and the DOS for $E \gg E_G$ are not related.

It is widely accepted that the Hubbard model describes the basic physics of the cuprates, e.g., Ref. [20] and references therein, but it has not been solved rigorously at low T and as far as we know does not account for points A–D above. Similar underlying physics occurs in the Friedel-Anderson model [21] and the Kondo effect [22,23] where metals, such as Cu or Au are alloyed with a small concentration ($c_{\rm imp}$) of magnetic elements (impurities), such as Fe or Mn. For both Kondo alloys and heavy fermion compounds, the electronic specific-heat coefficient $\gamma \equiv dS_e/dT$ is strongly enhanced at low T, in Wilson's solution of the Kondo problem [19], it is given by

$$\gamma_{\rm imp} = c_{\rm imp}\pi^2 k_B w/(6T_K), \qquad (1)$$

where T_K is the Kondo temperature and $w = 0.4128$ is the Wilson number. For impurities with spin 1/2, and $T \ll T_K$, $\chi_s^{imp} = c_{\rm imp}(g\mu_B)^2 w/(4k_B T_K)$, where $g \simeq 2$ is the g factor and $\chi_s^{imp}/\gamma_{\rm imp} = R_W = 2R_0$, in agreement with experiments on some Kondo alloys [23]. Here $R_0 = 3\mu_B^2/(\pi^2 k_B^2)$ is the Wilson ratio for non- or weakly interacting fermions.

For Bi2212, $\gamma(200)$ varies from 0.86 to 0.98 mJ/g at/K^2 for $0.095 < p < 0.22$ [2], and taking $c_{\rm imp}$ to be the concentration of Cu atoms, Eq. (1) gives a first estimate for $T_K \simeq 800$ K. We note that such a single-ion Kondo model works well for the heavy fermion compound $CePb_3$ doped with La [24]. For the same range of p, $\chi_s(200) = 2.18$–2.38×10^{-4} emu/mol Bi2212, see the footnote [25] giving a Wilson ratio $\chi_s/\gamma = 1.29$–$1.34R_0$. For $YBa_2Cu_3O_7$ where there is some uncertainty from the Cu-O chain contribution and in the precise value of $\gamma(300)$, $\chi_s/\gamma \simeq 1.2R_0$ [2,26]. So the experimental data is closer to R_0 rather than the Wilson value of $2R_0$. This is not a limitation because Fig. 10.9 of Ref. [23] shows that for heavy fermion compounds, such as $CeCu_2Si_2$, $CeCu_6$, and UPt_3, $\chi_s/\gamma \simeq R_0$, and as explained later, a ratio of 1.3 is consistent with the present picture. Numerical treatments of the t-J model [27], derived from the two-dimensional Hubbard model, give $\chi_s/\gamma \simeq R_0$ for $0.1 < p < 0.2$ and $T < J/k_B$. Large values of T_K do occur for dilute alloys, e.g., AlMn where $T_K = 600$ K at low T falling to 470 K near 300 K because of thermal expansion and the strong volume dependence of T_K [28]. This reduces the T dependence of $\chi_s(T)$ from the $1/(T + T_K)$ law usually found for alloys with lower T_K and less thermal expansion.

Here we consider three localized states, described by the asymmetric single orbital Anderson model. Figures 1(b) and 1(c), taken from Fig. 5 of Ref. [18], show the spectral density for an isolated ion obtained by numerical renormalization group (NRG) calculations for $E_0 = -U/2$, the symmetric case, and various asymmetric cases, $-E_0/\Delta = 4$, 3, and 2. $|E_0|$ and $U - |E_0| > 0$ are the energies required to transfer an electron from the singly occupied state to the Fermi level of the conduction electrons at E_F or from E_F to the doubly occupied state, respectively. U, set equal to $4\pi\Delta$ in Ref. [18], is the on-site d-d Coulomb repulsion, $\Delta = \pi V^2 N(E)$ [21], where V is the hybridization energy between the d state and the conduction electrons and $N(E)$ is their DOS for a given spin direction at the energy of the virtual bound state. The familiar triple peak structure in Fig. 1(b) has two side peaks arising from the localized level and a peak near E_F from the Kondo resonance. The weak-p dependence of γ and, hence, T_K for OD Bi2212 and other OD cuprates implies that E_0 and Δ are also only weakly dependent on p.

As originally shown by Kondo [29], the central peak is caused by the af exchange interaction $-2J_{\rm imp}\underline{S}_{\rm imp}\underline{s}_e$ with $J_{\rm imp} < 0$ between the spin on the magnetic ion, $\underline{S}_{\rm imp}$ and the spin of a conduction electron $\underline{s}_e$. The $S^+_{\rm imp}$ and $S^-_{\rm imp}$ operators do not commute, and because of this, higher-order scattering processes contain the Fermi function for the conduction electrons. This leads to the logarithmic Kondo divergence in the scattering rate, responsible for the resistance minimum observed in dilute magnetic alloys and for the formation of the Kondo resonance at E_F. It is a many-body effect because it depends on the occupancy of many other conduction electron states. The Kondo resonance has the same spatial symmetry as the electronic state of the localized level [22,30]. This is why band structures of heavy fermion materials, calculated using relatively standard methods, agree with the extremal orbits observed in quantum oscillation experiments, e.g., Ref. [31] because the band structures depend on this symmetry. But the effective masses (m^*) are often very large because they are determined by the energy width of the Kondo resonance. For the cuprates, this implies that the Fermi surface is large with the shape predicted by standard band theory, but m^* is larger.

The effects of an applied magnetic-field (H) and, more generally, an exchange field, are important here. In dilute Kondo alloys, H suppresses the Kondo effect because spin-flip scattering processes become inelastic in a magnetic field [22]. Early tunneling studies where a fraction of a monolayer of Fe atoms was evaporated on the oxide layer of an Al-Al_2O_3-Al junction [32] showed evidence for this "hole in the DOS," and it is indeed "non-states-conserving," see Fig. 9 of Ref. [32] shown in Fig. 5 of the SM [15]. Experimentally [33,34] and theoretically [35,36], this requires $\mu_B H \gtrsim k_B T_K$. A problem here is that such a large value of H, $\approx k_B T_K/\mu_B$, is incompatible with the appropriate condition $E_G \simeq \mu_B H$ when $p \lesssim p_{\rm crit}$ and E_G is small.

This difficulty is absent for a molecular field in NRG calculations [37] for the two-band Hubbard model plus a ferromagnetic predominantly Ising exchange interaction $-2J_{\rm ex}S_i^z s^z$ between the localized magnetic moments and the conduction electrons. Note that these calculations refer to a concentrated heavy fermionlike spin system. For $J_{\rm ex} = 0$, there are two side peaks from the narrow band, i.e., the localized magnetic states, and a central peak from the broad band, equivalent to the conduction electron band here. But as shown in Ref. [37] for large enough $J_{\rm ex}$, there is a quadruple peak in the DOS curves, i.e., an extra dip at E_F, whose width is $\simeq 2J_{\rm ex}$. It is possible that $J_{\rm ex}$ suppresses higher-order spin-flip scattering processes, thereby suppressing the DOS at E_F. There appears to be no limitation regarding the ratio of $J_{\rm ex}/k_B T_K$, in contrast to the effect of H on Kondo alloys. It is difficult to calculate Δ from first principles, even for noble-metal hosts, see Ref. [23], Chap. 9.7. We attempted this by calculating the band structure of the hypothetical compound $YBa_2Zn_3O_7$ in which all lattice parameters are kept the same as for $YBa_2Cu_3O_7$, using the WIEN2K code [38]. In a sense this is equivalent to experimentalists using Lu compounds with a full f shell as a reference for Yb compounds. The Brillouin zone is sketched in Fig. 6(a) of the SM [15] and dispersion curves shown in Fig. 6(b) of the SM [15]. The Zn d levels are well below E_F as shown by the DOS vs energy plots in Fig. 2 and there are approximately ten d states per Zn atom, i.e., a full d shell as expected from chemical arguments. In-plane states near E_F do have a small amount of d character, but as shown in Fig. 2, this is only a few percent of the DOS derived from the measured value of γ. In contrast, band-structure calculations for $YBa_2Cu_3O_7$ using the LDA give substantial contributions to $N(E_F)$ from the Cu $3d$ orbitals forming the Cu-O_2 plane bands. The full LDA DOS for $YBa_2Cu_3O_7$ (not shown) agrees well with earlier work [39], and $\gamma(300)$ is only moderately enhanced over the LDA value, see Fig. 2. But $N(E_F)$ from the in-plane oxygen bands and the in-plane Zn atoms in $YBa_2Zn_3O_7$ is much smaller, so in the present picture, the measured values of γ for YBCO and Bi2212 arise from the Kondo effect—Eq. (1). Figure 6(c) in the SM [15] shows the Fermi surface of $YBa_2Zn_3O_7$ with two quasicylindrical sheets of similar size from the bands crossing E_F between S and X and between S and Y, and an open surface from the band crossing E_F between Y and G. From Fig. 6(b) of the SM [15] the average value of E_F for the two quasicylindrical bands of the Zn compound is 0.54 eV relative to the top of the band. The average value of k_F in the S-X-Y plane is $0.35\,\pi/a$ where $a = 0.382$ nm is the in-plane lattice spacing, giving

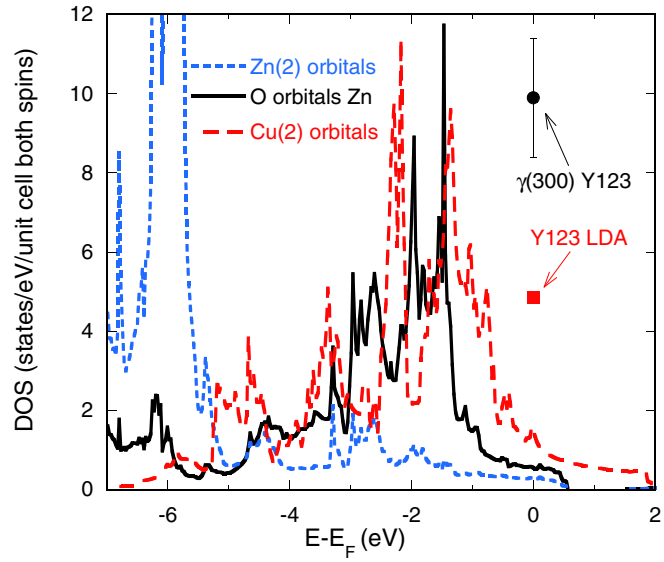

FIG. 2. Partial DOS vs energy E-E_F; in-plane oxygen orbitals of $YBa_2Zn_3O_7$, solid black line, d orbitals for Zn(2) atoms in $YBa_2Zn_3O_7$ and Cu(2) atoms in $YBa_2Cu_3O_7$, short and long dashed lines respectively. Points show $N(E_F)$ of $YBa_2Cu_3O_7$ from the local density approximation (LDA) and from $\gamma(300)$. When expressed as states/eV/Cu atom (both spins), $\gamma(300)$ for $YBa_2Cu_3O_7$, gives 3.3 ± 0.5, the same within errors as 2.9 ± 0.2 states/eV/Cu atom (both spins) from $\gamma(200)$ of Bi2212.

p for the two cylindrical bands which agrees well with the more precise value obtained by integrating the DOS plots in Fig. 2 for the in-plane O(2), O(3), and Zn(2) atoms. Namely, $p = 2 \times 0.19$/unit cell, in surprisingly good agreement with empirical experimental estimates for $YBa_2Cu_3O_7$ [40–42]. It would be interesting to see whether this procedure works for the two-chain compound $YBa_2Cu_4O_8$.

The complex band structure below ≈ -1 eV shown in Figs. 2 and 6(b) of the SM [15] prevents us estimating Δ from first principles, so initially, we set $\Delta = 1$ eV, a typical value for $3d$ impurities in noble metals [21,22]. But, as explained in more detail in the SM [15], we can account for the experimental value of the Wilson ratio if $E_0/\Delta = -2.3$ because for this value, linear interpolation of the data in Table 1 of Ref. [18] gives the occupancy of the localized level $n_0 = 0.81$ and an effective moment of $0.81\mu_B$. This reduces the susceptibility by 0.81^2 and the Wilson ratio from the value of 2 expected for an ion with $S = 1/2$ to 1.31, in good agreement with experiment. Theoretical $S_e(T)$ curves were obtained by integrating the specific-heat data in Fig. 4 of Ref. [18] divided by T. For $T_K = 800$ K, γ increases by a factor of 1.19 between $T = 200$ K and $T = 0$, so the initial estimate of $T_K = 800$ K from $\gamma(200)$ of Bi2212 is reduced to 672 K. Theoretical curves for representative samples of Bi2212, one with no PG $p = 0.19$, and one with a PG, are linear over the measured range of $T \leqslant 220$ K as shown in Fig. 7 of the SM [15]. In contrast, those for $YBa_2Cu_3O_{6.97}$ with no PG and $YBa_2Cu_3O_{6.48}$ with $E_G/k_B = 320$ K, in Fig. 8 of the SM [15], both having $T_K = 775$ K, show deviations from linearity above 200 K. But these do not rule out the present picture because they could arise from a modest decrease in T_K caused by thermal expansion or

because the Cu atoms in the CuO chains and the CuO_2 planes are inequivalent.

Hence, for Bi2212 $T_K = 672$ K and for $E_0/\Delta = -2.3$, $k_BT_K/\Delta = 0.073$, and $\Delta = 0.79$ eV. The observation of significant g-factor anisotropy in YBCO [6] and references therein, supports the present localized picture. Here the concept of valency is meaningful, the Cu^{2+} (d^9) state will be dominant, and for $-E_0 = 2.3\Delta$, there is a certain admixture of Cu^{3+} (d^8). The d^{10} and d^9 states are analogous to those in heavy fermion Yb compounds with 0 or 1 hole in the $4f$ shell, which implies that all the Cu d electrons are contributing to U. As shown in Fig. 1(c), the half width half maximum (HWHM) values of the spectral density at $\omega < 0$ for $-E_0/\Delta = 3$ and 2 are $\simeq 0.076\Delta$ and 0.135Δ, respectively, giving 0.117Δ for $-E_0/\Delta = 2.3$. The carrier density in the resonance n_K, obtained by assuming that it has a Lorentzian shape for $\omega < 0$ and normalizing to the area of the lowest broad peak in Fig. 1(b) that contains $\simeq 1$ electron, agrees well with $(1\text{-}n_0)/2 = 0.095$. For $\Delta = 0.79$ eV the HWHM is $T_L = 1072$ K. When transformed in the usual way into $\underline{k}$ and then by Fourier transform into $\underline{r}$ space, *and in the absence of a PG*, the carrier density decays as $n_K \exp(-r/R)$ with a range of $R = \frac{\hbar v_F}{k_B T_L}$. The resonance is centered at the Fermi level and because of the sharpness of the Fermi surface, the Fourier transform could also give rise to Friedel- or Rudermann-Kittel-Kasuya-Yosida-type oscillations in $n_k(r)$, that could also be important but are not considered here. The Fermi velocity $v_F = 1.6\,10^7$ cm/sec, estimated for a cylindrical surface containing $1+p$ holes with $m^* = 5.2m_e$ [43], agrees well with nodal ARPES data for UD and optimally doped (OP) crystals of the single-layer cuprate Hg1201 shown in Fig. 2(b) of Ref. [44], 1.7, 2.2, and 2.0×10^7 cm/s for UD70, UD80, and OP98. This agreement supports our statement that T_K and, hence, m^* vary little with p.

The above values of v_F and T_L give $R = 2.83a$. From the previous spatial symmetry argument, n_K will have $|d_{x^2-y^2}|$ symmetry and be larger in the (0,1) and (1,0) directions, where af spin fluctuations cause neighboring spins to be antiparallel over a certain spatial range of ξ. A typical value for $p = 0.1$ is $\xi = 0.9$ nm, i.e., 2-3a [14]. If $\xi = 2a$, then only the four nearest neighbors have correlated spins. Their af Kondo screening "clouds" will give a *ferromagnetic* conduction electron spin polarization at the central site. Including the effect of the PG on both n_k and R (by self-consistently representing the PG by a narrower negative Lorentzian) reduces n_k at the central site by a factor of $\simeq 2$, giving a magnetic moment from the four overlapping Kondo "clouds" of $2 \times 0.095 \times \exp(-1/2.83)\mu_B = 0.133\mu_B$. It is difficult to prove that this spin polarization is equivalent to $J_{\rm ex}$ in Ref. [37], but for $\chi_s = 2.3 \times 10^{-4}$ emu/mol-2212, a spin polarization of $0.133\mu_B$/Cu is produced by a field H where $\mu_B H/k_B = 433$ K, so $J_{\rm ex}/k_B = 866$ K. From Fig. 2 of Ref. [37] the half energy gap, equivalent to E_G here, is $\simeq J_{\rm ex}$, in reasonable agreement with the experimental value $E_G/k_B \simeq 600$ K for $p = 0.1$. Furthermore, the imaginary part of the self-energy is unusual and typical of a "bad metal" [37] in agreement with experiments on the cuprates. However, more work is needed to see whether $J_{\rm ex}$ falls linearly with p and whether calculations allowing for asymmetry in the DOS about E_F on a scale of $J_{\rm ex}$, i.e., E_G, would account for the strong p dependence of the TEP and its scaling with k_BT/E_G [11,26], shown in Fig. 9 of the SM [15].

Alternatively, in a related picture, the effect of the af fluctuations, i.e., the interactions between neighboring Cu spins, could be considered directly, without appealing to the work of Ref. [37]. These will reduce the entropy of the Cu spins and, hence, that available for the Kondo resonance. Key theoretical questions are as follows: (a) can they cause a deep PG even when the interaction energy (W) is much smaller than k_BT_K, and (b) does W fall linearly with p and become very small for $p \geqslant p_{\rm crit}$? Experimental evidence for (b) is given by ratio of the ^{63}Cu and ^{17}O NMR relaxation rates T_1^{-1} [9] which is a measure of the strength of low-frequency spin fluctuations for which the effect of the PG on χ_s cancels out. It does, indeed, fall linearly with p, approaching zero at $p_{\rm crit}$. Analysis [45] of neutron-scattering data shows the same decrease for af spin fluctuations of energy below 50 meV, so on the timescale of the Kondo resonance with $k_BT_K \approx 60$ meV, they will provide a molecular field that is nearly static.

Within the usual localized picture, W arises from superexchange via completely occupied or completely empty oxygen $2p$ states. For a band with Fermi energy E_F, we should consider Wannier functions that have a lifetime on the order of $\hbar/E_F$. E_F will increase with p, thereby reducing W, which could account for point (b) above. As sketched for example in Fig. 13 of Ref. [26], only those parts of the large Fermi surface spanned by the af wave-vector $\underline{Q} \approx (\frac{\pi}{a}, \frac{\pi}{a})$ will be affected by af fluctuations. This accounts for the Fermi arcs, where $E_G = 0$, seen by ARPES [46] and scanning tunneling microscopy (STM) [47]. It also gives a strong energy dependence of the scattering rate responsible for the TEP [26], see also Ref. [48], and its scaling with k_BT/E_G shown in Ref. [26] and Fig. 9 of the SM [11,15].

Evidence for an energy scale $\approx$60 meV in the many spectroscopic studies of cuprates above T_c would be a good experimental test of the present picture. ARPES data do show structures near 50 meV, e.g., Ref. [44] that is presently ascribed to other factors. However, we are dealing with a many-body effect, so comparison of ARPES, STM [47], and optical data [49,50] for cuprates with those for heavy fermion compounds as well as with theory could be informative. Another test would the apparent correlation between the T^1 term in the electrical resistivity and the superfluid density [51] in OD compoumds. One prediction of the present approach is that m^* and related properties of OD Tl2201 crystals could be strongly pressure dependent since for classical Kondo alloys the volume (V) dependence of T_K is large, $-d \ln T_K/d \ln V = 16$–18 [28,52].

To summarize, guided by the unusual behavior of the electronic entropy revealed by specific-heat measurements [1,2,10], we propose that the pseudogap is the energy scale over which a Kondo-like enhanced DOS at the Fermi energy is suppressed by af spin interactions.

I would like to thank A. Carrington, who also calculated the band structure of $YBa_2Zn_3O_7$, J. L. Tallon, and V. Zlatić for helpful suggestions and discussions and to acknowledge a long and happy collaboration with the late Dr. J. W. Loram.

[1] J. W. Loram, K. A. Mirza, J. R. Cooper, and J. L. Tallon, Specific heat evidence on the normal state pseudogap, J. Phys. Chem. Solids **59**, 2091 (1998).

[2] J. W. Loram, J. Luo, J. R. Cooper, W. Y. Liang, and J. L. Tallon, Evidence on the pseudogap and condensate from the electronic specific heat, J. Phys. Chem. Solids **62**, 59 (2001).

[3] W. Anukool, S. Barakat, C. Panagopoulos, and J. R. Cooper, Effect of hole doping on the London penetration depth in $Bi_{2.15}Sr_{1.85}CaCu_2O_{8+\delta}$ and $Bi_{2.1}Sr_{1.9}Ca_{0.85}Y_{0.15}Cu_2O_{8+\delta}$, Phys. Rev. B **80**, 024516 (2009).

[4] J. R. Cooper, J. W. Loram, J. D. Johnson, J. W. Hodby, and C. Changkang, 3D XY Scaling of the Irreversibility Line of $YBa_2Cu_3O_7$ Crystals, Phys. Rev. Lett. **79**, 1730 (1997).

[5] B. Keimer, S. A. Kivelson, M. R. Norman, S. Uchida, and J. Zaanen, From quantum matter to high-temperature superconductivity in copper oxides, Nature (London) **518**, 179 (2015).

[6] I. Kokanović and J. R. Cooper, Magnetic susceptibility of $YBa_2Cu_3O_{6+x}$ crystals: Unusual Curie behavior and small contributions from charge density waves, Phys. Rev. B **94**, 075155 (2016).

[7] R. Comin, A. Frano, M. M. Yee, Y. Yoshida, H. Eisaki, E. Schierle, E. Weschke, R. Sutarto, F. He, A. Soumyanarayanan, Y. He, M. Le Tacon, I. S. Elfimov, J. E. Hoffman, G. A. Sawatzky, B. Keimer, and A. Damascelli, Charge order driven by Fermi-arc instability in $Bi_2Sr_{2-x}La_xCuO_{6+\delta}$, Science **343**, 390 (2014).

[8] Y. Sato, S. Kasahara1, H. Murayama, Y. Kasahara, E.-G. Moon, T. Nishizaki, T. Loew, J. Porras, B. Keimer, T. Shibauchi, and Y. Matsuda, Thermodynamic evidence for a nematic phase transition at the onset of the pseudogap in $YBa_2Cu_3O_y$, Nat. Phys. **13**, 1074 (2017).

[9] J. L. Tallon and J. W. Loram, The doping dependence of T* - what is the real high-T-c phase diagram?, Physica C **349**, 53 (2001).

[10] J. W. Loram, K. A. Mirza, J. R. Cooper, and W. Y. Liang, Electronic Specific Heat of $YBa_2Cu_3O_{6+x}$ from 1.8 to 300 K, Phys. Rev. Lett. **71**, 1740 (1993).

[11] J. R. Cooper, H. Minami, V. W. Wittorff, D. Babić, and J. W. Loram, Effect of the normal state gap on the thermoelectric power, irreversibility line and c-axis resistivity of $YBa_2Cu_3O_{7-\delta}$, Physica C **341**, 855 (2000).

[12] G. V. M. Williams, J. L. Tallon, R. Michalak, and R. Dupree, NMR studies of overdoped $Y_{1-x}Ca_xBa_2Cu_3O_{7-\delta}$, Phys. Rev. B **57**, 8696 (1998).

[13] S. Kawasaki, C. T. Lin, P. L. Kuhns, A. P. Reyes, and G. Zheng, Carrier-concentration dependence of the pseudogap ground state of superconducting $Bi_2Sr_{2-x}La_xCuO_{6+\delta}$ revealed by Cu-63, Cu-65-Nuclear Magnetic Resonance in Very High Magnetic Fields, Phys. Rev. Lett. **105**, 137002 (2010).

[14] J. Rossat-Mignod, L. P. Regnault, C. Vettier, P. Bourges, P. Burlet, J. Bossy, J. Y. Henry, and G. Lapertot, Spin dynamics in the high T_c system $YBa_2Cu_3O_{6+x}$, Physica B **180-181**, 383 (1992).

[15] See Supplemental Material at http://link.aps.org/supplemental/10.1103/PhysRevB.105.L041102 for additional figures, explanations and References [55–57].

[16] J. Nachtigal, M. Avramovska, A. Erb, D. Pavićević, R. Guehne, and J. Haase, Temperature-independent cuprate pseudogap from planar oxygen NMR, Condens. Matter **5**, 66 (2020).

[17] S. H. Naqib, J. R. Cooper, and J. W. Loram, Effects of Ca substitution and the pseudogap on the magnetic properties of $Y_{1-x}Ca_xBa_2Cu_3O_{7-\delta}$, Phys. Rev. B **79**, 104519 (2009).

[18] T. A. Costi, A. C. Hewson, and V. Zlatić, Transport coefficients of the Anderson model via the numerical renormalization group, J. Phys.: Condens. Matter **6**, 2519 (1994).

[19] K. G. Wilson, Renormalization group- critical phenomena and Kondo problem, Rev. Mod. Phys. **47**, 773 (1975).

[20] W. Wu, M. S. Scheurer, S. Chatterjee, S. Sachdev, A. Georges, and M. Ferrero, Pseudogap and Fermi-Surface Topology in the Two Dimensional Hubbard Model, Phys. Rev. X **8**, 021048 (2018).

[21] P. W. Anderson, Localized magnetic states in metals, Phys. Rev. **124**, 41 (1961).

[22] G. Grüner, Experimental evidence for many-body effects in dilute alloys, Adv. Phys. **23**, 941 (1974).

[23] A. C. Hewson, *The Kondo Problem to Heavy Fermions* (Cambridge University Press, Cambridge, UK, 1993).

[24] C. L. Lin, A. Wallash, J. E. Crow, T. Mihalisin, and P. Schlottmann, Heavy-Fermion Behavior and the Single-ion Kondo Model, Phys. Rev. Lett. **58**, 1232 (1987).

[25] The measured susceptibility of Bi2212 at 300 K, is 1.1–1.3 emu/mole-Bi2212 [2] for $0.095 < p < 0.22$, giving $\chi_s = 2.18$–2.38×10^{-4} emu/mol-Bi2212 after corrections for core diamagnetism and Van Vleck orbital paramagnetism. These are -1.95×10^{-4} emu/mol-Bi2212 [53] and 0.866×10^{-4} emu/mol-Bi2212, respectively, using the Cu-O_2 plane value for YBCO [54].

[26] J. R. Cooper and J. W. Loram, Some correlations between the thermodynamic and transport properties of high T_c oxides in the normal state, J. Phys. I (France) **6**, 2237 (1996).

[27] J. Jaklić and P. Prelovšek, Finite-temperature properties of doped antiferromagnets, Adv. Phys. **49**, 1 (2000).

[28] J. R. Cooper and M. Miljak, Single impurity behaviour and interaction effects in the magnetic susceptibility of AlMn and AlCr alloys, J. Phys. F: Met. Phys. **6**, 2151 (1976).

[29] J. Kondo, Resistance minimum in dilute magnetic alloys, Prog. Theor. Phys. **32**, 37 (1964).

[30] A. Blandin, Magnetic impurities in metals, J. Appl. Phys. **39**, 1285 (1968).

[31] A. Pourret, M.-T. Suzuki, A. P. Morales, G. Seyfarth, G. Knebel, D. Aoki, and J. Flouquet, Fermi surfaces in the antiferromagnetic, paramagnetic and polarized paramagnetic states of $CeRh_2Si_2$ compared with quantum oscillation experiments, J. Phys. Soc. Jpn. **86**, 084702 (2017).

[32] S. Bermon, D. E. Paraskevopoulos, and P. M. Tedrow, Ultra-high magnetic field study of the Kondo-type zero-bias conductance peak in magnetically doped metal-insulator-metal tunnel junctions, Phys. Rev. B **17**, 2110 (1978).

[33] P. Monod, Magnetic Field Dependence of the Kondo Resistivity Minimum in CuFe and CuMn Alloys, Phys. Rev. Lett. **19**, 1113 (1967).

[34] H. Rohrer, High-field magnetoresistance of dilute Cu-Mn and Cu-Fe alloys, J. Appl. Phys. **40**, 1472 (1969).

[35] B. Horvatić and V. Zlatić, Magnetic field effects for the asymmetric Anderson Hamiltonian, Phys. Rev. B **30**, 6717 (1984).

[36] T. A. Costi, Kondo Effect in a Magnetic Field and the Magnetoresistivity of Kondo Alloys, Phys. Rev. Lett. **85**, 1504 (2000).

[37] T. A. Costi, and A. Liebsch, Quantum Phase Transition in the Two-Band Hubbard Model, Phys. Rev. Lett. **99**, 236404 (2007).

[38] P. Blaha, K. Schwarz, G. K. H. Madsen, D. Kvasnicka, J. Luitz, R. Laskowski, F. Tran, and L. D. Marks, *WIEN2K, An Augmented Plane Wave + Local Orbitals Program for Calculating Crystal Properties* (Vienna University of Technology, Austria, 2021).

[39] W. E. Pickett, Electronic structure of the high-temperature oxide superconductors, Rev. Mod. Phys. **61**, 433 (1989).

[40] M. R. Presland, J. L. Tallon, R. G. Buckley, R. S. Liu, and N. E. Flower, General trends in oxygen stoichiometry on T_c in Bi and Tl superconductors, Physica C **176**, 95 (1991).

[41] R. Liang, D. A. Bonn, and W. N. Hardy, Evaluation of CuO_2 plane hole doping in $YBa_2Cu_3O_{6+x}$ single crystals, Phys. Rev. B **73**, 180505(R) (2006).

[42] S. D. Obertelli, J. R. Cooper, and J. L. Tallon, Systematics in the thermoelectric power of high T-c oxides, Phys. Rev. B **46**, 14928(R) (1992).

[43] A. F. Bangura, P. M. C. Rourke, T. M. Benseman, M. Matusiak, J. R. Cooper, N. E. Hussey, and A. Carrington, Fermi surface and electronic homogeneity of the overdoped cuprate superconductor $Tl_2Ba_2CuO_{6+\delta}$ as revealed by quantum oscillations, Phys. Rev. B **82**, 140501(R) (2010).

[44] S. A. Sreedhar, A. Rossi, J. Nayak, Z. W. Anderson, Y. Tang, B. Gregory, M. Hashimoto, D.-H. Lu, E. Rotenberg, R. J. Birgeneau, M. Greven, M. Yi, and I. M. Vishik, Three interaction energy scales in the single-layer high-Tc cuprate $HgBa_2CuO_{4+\delta}$, Phys. Rev. B **102**, 205109 (2020).

[45] J. G. Storey, J. L. Tallon, and G. V. M. Williams, Pseudogap ground state in high temperature superconductors, Phys. Rev. B **78**, 140506(R) (2008).

[46] S. Chen, M. Hashimoto, Y. He, D. Song, K.-J. Xu, J.-F. He, T. P. Devereaux, H. Eisaki, D.-H. Lu, J. Zaanen, and Z.-X. Shen, Incoherent strange metal sharply bounded by a critical doping in Bi2212, Science **366**, 1099 (2019).

[47] K. Fujita, C. K. Kim, I. Lee, J. Lee, M. H. Hamidian, I. A. Firmo, S. Mukhopadhyay, H. Eisaki, S. Uchida, M. J. Lawler, E.-A. Kim, and J. C. Davis, Simultaneous transitions in cuprate momentum-space topology and electronic symmetry breaking, Science **344**, 612 (2014).

[48] G. Hildebrand, T. J. Hagenaars, W. Hanke, S. Grabowski, and J. Schmalian, Effects of electronic correlations on the thermoelectric power of the cuprates, Phys. Rev. B **56**, R4317 (1997).

[49] D. N. Basov and T. Timusk, Electrodynamics of high-T_c superconductors, Rev. Mod. Phys. **77**, 721 (2005).

[50] S. Tajima, Optical studies of high-temperature superconducting cuprates, Rep. Prog. Phys. **79**, 094001 (2016).

[51] M. Čulo, C. Duffy, J. Ayres, M. Berben, Y.-T. Hsu, R. D. H. Hinlopen, B. Bernáth, and N. E. Hussey, Possible superconductivity from incoherent carriers in overdoped cuprates, SciPost Phys. **11**, 012 (2021).

[52] J. S. Schilling and W. B. Holzapfel, Effect of pressure on the Kondo temperature of Cu:Fe-existence of a universal resistivity curve, Phys. Rev. B **8**, 1216 (1973).

[53] P. W. Selwood, *Magnetochemistry*, 2nd ed. (Interscience, New York, London, 1956).

[54] F. Mila and T. M. Rice, Analysis of magnetic resonance experiments in $YBa_2Cu_3O_7$, Physica C **157**, 561 (1989).

[55] H.-U. Desgranges and K. D. Schotte, Specific heat of the Kondo model, Phys. Lett. A **91**, 240 (1982).

[56] V. T. Rajan, Magnetic Susceptibility and Specific Heat of the Coqblin-Schrieffer Model, Phys. Rev. Lett. **51**, 308 (1983).

[57] J. W. Loram, K. A. Mirza, and J. R. Cooper, *IRC Research Review*, edited by W. Y. Liang (University of Cambridge, Cambridge, UK, 1998), pp. 75–97.